

## DEGRADATION MECHANISMS OF MAGNESIA-CHROMITE REFRACTORIES IN VOD-LADLES AND MEASURES TO EXTEND THE LINING LIFE

P.T. Jones\*, B. Blanpain\*, P. Wollants\*, R. Ding\*<sup>‡</sup>,  
B. Halleman\*, J. Weytjens\*\* and G. Heylen\*\*

\*K.U.LEUVEN (department MTM), Leuven, Belgium, \*\*ALZ, Genk, Belgium

### ABSTRACT

Magnesia-chromite bricks are used as refractories for the refining of stainless steels in VOD-ladles at the ALZ Company. Refractory wear is not uniform. Bricks from different degraded zones in the ladle were analysed with EPMA-EDS. The refractory wear, as a function of the position in the ladle, is shown. The potential negative effect of the presence of FeO<sub>x</sub> in magnesia-chromite refractories is demonstrated.

Different but related degradation mechanisms are proposed: slag infiltration and MgO-dissolution, continuous wear due to hot erosion of partially liquid-bonded refractories, discontinuous wear due to spalling and cracking. Finally, a method to extend the refractory life is presented.

### I. INTRODUCTION

The ALZ Company uses a VOD-installation for the secondary refining of high quality stainless steel grades. High density direct-bonded magnesia-chromite bricks are used as main refractory material in the ladle. The as-delivered material (nominal composition by weight: 57-60% MgO, 18.5-21% Cr<sub>2</sub>O<sub>3</sub>, 13-13.5% Fe<sub>2</sub>O<sub>3</sub>, 5.5-6.5% Al<sub>2</sub>O<sub>3</sub>, 1.2% CaO and 0.5% SiO<sub>2</sub>) consists of magnesia, chromite spinel and silicate phases (see **Fig. 1**). The chromite is present as large (> 0.2 mm) crystals (primary spinel) and small grains (secondary spinel). There are two types of secondary spinel. Type I arises via precipitation on cooling and forms at magnesia grain boundaries, exsolved out of magnesia (Ia) or crystallised from chromia-rich liquid (Ib). Type II arises from exsolution precipitation from magnesia grains on cooling and forms within these magnesia grains.<sup>1</sup> The silicate phase (i.e. C<sub>2</sub>S) cannot be seen on the SEM-micrograph (**Fig. 1**) of the as-delivered magnesia-chromite refractory, as this phase is largely removed during sample preparation, due to the dusting phenomenon.

Several studies on the wear mechanisms of magnesia-chromite refractories have been published. Mosser *et al.*<sup>2</sup> have described the degradation of magnesia-chromite bricks in RH-degassers. They observe that the wear is primarily characterised by the infiltration of silicate-rich slags into pores, reaction of the infiltrate with the matrix of the brick and subsequent hot erosion of the infiltrated zone. The densified zone tends to peel off in the transition zone to the non-infiltrated area.<sup>2</sup> Engel *et al.*<sup>3</sup> have compared the wear mechanisms of magnesia-chromite with those of magnesia-doloma refractories. Spinel minerals can be dissolved by slags with high lime content and are reduced more readily. The successful use of magnesia-chromite refractories often requires the use of MgO-saturated slags containing more than 15 wt-% MgO, as reported by Engel *et al.*<sup>3</sup>

In this paper we report on the chemical interactions between magnesia-chromite refractories and liquid phases, and on the influence of the ferrostatic pressure and the process temperature on the refractory wear. A set of interdependent degradation mechanisms is proposed and the refractory

<sup>‡</sup> Current address: Queen Mary and Westfield College, London, UK

wear, as a function of the position in the ladle, is shown. Finally, a method to extend the refractory life is presented.

## II. PROCESS INFORMATION AND EXPERIMENTAL PROCEDURES

### A. *The VOD-process*

The VOD-process consists of three stages: blowing, degassing and reduction. In the blowing stage, oxygen is added to the melt to lower the carbon level to 0.005-0.1 wt-%, depending on the steel grade. The total pressure in the gas phase is approximately 0.1 to 0.2 atm. It is important to control the processing conditions to minimise chromium losses during the blow. Towards the end of the blowing stage, the slag consists of a mixture of solid  $\text{CrO}_x$  and a liquid phase saturated with  $\text{CrO}_x$ . The processing temperature during this stage can be as high as 1750°C, occasionally exceeding this value. In the degassing stage the total pressure is reduced to approximately 0.001-0.005 atm. Finally, during the reduction phase, ferrosilicon (in combination with smaller amounts of aluminium) is added to the melt to recover the chromium from the slag.

### B. ALZ's VOD-ladle lining

ALZ uses VOD-ladles with a capacity of 120 tons of steel. Two types of high quality direct-bonded magnesita-chromite refractories are used as working lining in the metal bath zone and in the slag line. Lower quality dolomite bricks are installed in the upper layers of the working lining, whereas the ladle bottom consists of magnesita-carbon refractories. The bricks in the upper lining and in the bottom of the ladle are barely degraded during the VOD-process and therefore will not be discussed. The average slag weight varies between 3 to 5 tons. The degradation of the refractories is not uniform. The average wear in the bottom rows of the ladle is rather limited, whereas bricks in contact with the slag and the refractories in the upper rows of the metal bath are severely degraded.

### C. The materials

Over a period of two years several post-mortem analyses were done, mainly on bricks from the slag area. To get an overall (interrelated) picture of the refractory breakdown mechanisms, worn bricks were taken from different rows from one specific VOD-ladle. This procedure was repeated for different VOD-ladles. In this paper we report on common phenomena. An overview of the different sample bricks of one particular ladle - which is considered as representative for other worn VOD-ladles at ALZ - is given in **Table 1**. Of each brick several SEM-samples were prepared (hot face, cold face...). The samples were cut with a diamond saw, embedded in resin (Technovit 4004), and ground with SiC grit. Finally, carbon was evaporated on the sample surface to provide a conducting layer.

### D. Techniques

Most of the chemical analyses were done with a JEOL 733 electron probe microanalysis system equipped with an energy dispersive spectroscopy system (Be window) from Tracor. The composition was determined using a standardless quantification routine SQ provided by Tracor

(EPMA-EDS, electron beam conditions: 15 kV, 20 nA). The oxygen content is calculated through the measured element signals (*e.g.* Fe) and the *a priori* selected oxides (*e.g.* FeO or Fe<sub>2</sub>O<sub>3</sub>). The Fe-state was chosen for each measurement with consideration of its specific circumstances. Finally, wet chemical analyses of slag samples were carried out with a VARIAN Liberty Series II axial Inductively Coupled Plasma Atomic Emission Spectroscopy (ICP-AES) instrument.

### III. RESULTS AND DISCUSSION

#### A. Overview of main results for different samples

**Fig. 2** shows a SEM-micrograph of the hot face of the S4-brick. **Table 2** summarises the main characteristics of the samples of **Table 1**, as determined with the JEOL 733 microscope. Wear was severe in the bricks in contact with the slag zone (S4 and S5) and in the bricks in the upper metal bath rows of the ladle (S3). This degradation is characterised by slag infiltration and MgO-dissolution, the formation of metallic particles originating from FeO<sub>x</sub>- (and some Cr<sub>2</sub>O<sub>3</sub>-) decomposition, and degradation of primary chromite.

#### B. Slag infiltration and refractory dissolution

In general, the samples taken from the worn bricks contained a slag infiltrated zone (0.5 to 5 cm deep) and a non-infiltrated zone in the interior of the brick. Some samples had a slag layer on their surface (*e.g.* see **Fig. 2**). The slag infiltrated zone can be subdivided into two areas: a metallic droplets (10-30 µm, mainly Fe) containing part at the hot face and a metal-free slag infiltrated zone. Severe slag infiltration occurred in S3, S4 and S5 essentially via magnesia grain boundaries, as the ability of a liquid phase to penetrate between unlike grains (*e.g.* spinel-magnesia) is less than between like grains (*e.g.* magnesia-magnesia).<sup>4</sup> The amount of slag infiltration is not only determined by the position of the brick in the ladle (*e.g.* difference S1/S4, **Table 2**), but also by the processing temperature, the oxygen partial pressure, the holding time of the melt in the ladle, the slag composition and viscosity (determining the slag aggressiveness) and finally the temperature gradient in the brick. Infiltrating silicate slags that are not MgO-saturated pick up and dissolve MgO from the refractory at the hot face of the brick. The slag phase chemistry thus changes from the C<sub>2</sub>S/C<sub>3</sub>MS<sub>2</sub> to the C<sub>3</sub>MS<sub>2</sub>/CMS region in the CaO-SiO<sub>2</sub>-MgO system.<sup>5</sup> Slag that penetrates deeper in the brick slowly solidifies without much reaction with the refractory, due to the lower temperatures in the interior of the brick that create kinetic restrictions. This explains why the worn bricks contain large amounts of CMS at the hot face, whereas deeper in the brick both CMS and C<sub>3</sub>MS<sub>2</sub> are found. In the interior of the incompletely infiltrated bricks (S1, S2 and S6), no CMS or C<sub>3</sub>MS<sub>2</sub> is detected. The latter phases cause serious problems in the infiltrated areas of the brick. Both phases have lower melting temperatures (CMS: T<sub>m</sub> ≈ 1500°C, C<sub>3</sub>MS<sub>2</sub>: T<sub>m</sub> ≈ 1575°C) than the original C<sub>2</sub>S-silicate phase (T<sub>m</sub> ≈ 2130°C), and subsequently diminish refractoriness of the brick.<sup>6</sup> The microstructure of the original refractory material is characterised by a high proportion of direct bonding between the MgO-matrix and the chromite, *i.e.* a direct attachment of magnesia to chromite without any interrupting film of silicate.<sup>1</sup> Especially the secondary chromite provides for this direct bonding. However, when magnesia-

chromite refractories are used in VOD-ladles at elevated temperatures, normal direct bonding is disturbed:

- 1) Infiltration of the liquid silicate slag through the open pore network and via the magnesia grain boundaries decreases the direct bonding between magnesia grains. Furthermore, MgO from the magnesia grains is dissolved into the MgO-undersaturated slag.
- 2) The secondary chromite, which is supposed to prevent slag infiltration by providing for magnesia-spinel direct bonding, is partially ‘inactivated’. Firstly, in highly degraded samples (e.g. S4, see **Fig. 2**) secondary spinel type Ia and type II are only present in minor amounts at the hot face of the brick. They are essentially (re)dissolved, via diffusion mechanisms activated by the high VOD-processing temperatures, into the surrounding magnesia. Secondly, the secondary spinel type Ib is to some extent dissolved into the liquid silicate phase.<sup>7</sup> **Fig 2** indeed shows that the secondary chromite phase (type Ib) occasionally coexists with a silicate phase, indicating that this spinel phase was partially liquid at steelmaking temperatures and that it has precipitated/crystallised from a chrome-rich liquid during cooling (e.g. the temperature in the slag-line refractories slowly decreases with approximately 200°C between the end of the blowing stage and the beginning of continuous casting).

Both processes strongly decrease the amount of normal direct bonding in the brick, partially replacing it with liquid bonding (*i.e.* a chrome-rich liquid silicate phase). Turbulent bath movement during the blowing stage easily erodes such a partially liquid bonded system. This erosion mechanism is intensified at the slag/metal interface by strong (local) turbulent currents, induced by the Marangoni-effect.<sup>8</sup> The amount of erosion is directly proportional to the temperature of the liquid phases in contact with the refractories (see **Fig. 3**).

A co-operating degradation mechanism is discontinuous wear due to spalling. The net result of severe slag infiltration is densification of the brick near the hot face. The densified zone has a different expansion behaviour than the non-infiltrated zone, resulting in high internal stresses, leading to crack formation and spalling.

Refractory dissolution into the liquid slag was confirmed by comparing EPMA-EDS data with results obtained through wet chemical analysis using ICP-AES. It was established that the MgO-content of the slag increased from an initial theoretical value (*i.e.* the estimated value based on slag additions, carry-over convertor slag and slag left over from a previous melt) of approximately 7.0 wt-% to a final value of 9.4 wt-%. The latter value was determined by ICP-AES analysis of a slag sample taken at the end of the VOD-reduction stage. The slag phases found on samples S4 and S5, were representative of the ‘sticky’ slag left behind on the refractory bricks when continuous casting commenced. **Table 3** shows the EPMA-EDS results for the slag on sample S4. This composition was confirmed by the result for the slag on sample S5. The increase in MgO-content from 9.4 to 11.3 wt-% was the result of the further corrosion of refractory by slag between the end of the VOD-reduction stage and the beginning of the continuous casting. This indicates that the MgO-concentration of the slag tends towards its saturation value for MgO, as also reported by Engel *et al.*<sup>9</sup>

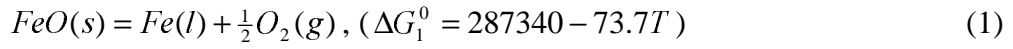
### C. FeO<sub>x</sub>-decomposition

The hot faces of samples S1-S6 were analysed to determine their FeO<sub>x</sub>-concentration as a function of their position in the ladle. The results were produced with large (covering 25 mm<sup>2</sup>) sample scans. The FeO-values of the hot faces in the worn bricks (**Table 1**) are considerably

lower than the nominal  $\text{FeO}_x$ -content of the as-delivered material ( $\sim 13$  wt-%). One obvious reason is the dilution effect caused by slag infiltration (mainly  $\text{CaO}$  and  $\text{SiO}_2$ ). For samples S3, S4 and S5 a high proportion of the calculated  $\text{FeO}$  is in fact present as metallic  $\text{Fe}$  (see **Fig. 2**). Although the signal height for an equal amount of  $\text{Fe}$ , present as either  $\text{FeO}$  or metallic  $\text{Fe}$ , is slightly different, the low values for S3, S4 and S5 (**Table 1**) indicate that the total  $\text{Fe}$ -amount in the hot face has decreased significantly. The overall trend shown in **Fig. 4** was confirmed by analyses of other VOD-ladles. The  $\text{FeO}_x$ -decomposition reaction apparently only occurs if two conditions are met simultaneously: high temperature and low oxygen partial pressure. That explains why samples S3, S4 and S5 contain metallic particles, whereas samples S1 (high temperature, but also high ferrostatic pressure) and S6 (higher oxygen partial pressure, lower temperature and no permanent contact refractory/melt) do not. **Fig. 4** thus shows that the influence of the ferrostatic pressure, which is directly related to the position of the brick in the ladle, cannot be disregarded. The total pressure ( $p_{t,h}$ ) at depth  $h$  in the ladle is:

$$p_{t,h} = p_{vac} + p_{Fe,h}$$

where  $p_{vac}$  is the total pressure in the gas phase, which is the sum of the partial pressures of  $\text{Ar}$ ,  $\text{CO}$ ,  $\text{CO}_2$  and  $\text{O}_2$ , and  $p_{Fe,h}$  is the ferrostatic pressure ( $\rho_s g h$ ). During the blowing stage  $p_{vac}$  is approximately 0.1 to 0.2 atm, whereas during the reduction stage it is lower ( $1\text{--}5 \cdot 10^{-3}$  atm). Consider the reaction:



where  $\Delta G_1^0$  is the standard reaction free energy in J.<sup>10</sup>  $\text{Fe}_2\text{O}_3$  is also present, dissolved in both the magnesia and the chromite phases, but for the sake of simplicity only the decomposition of  $\text{FeO}$  is considered here. The concentration of oxygen dissolved in the melt and the temperature for the different process stages (blowing, degassing and reduction stage) were calculated with a mathematical model for the VOD-process.<sup>11</sup> In order to calculate the oxygen partial pressure in the gas phase, we assume that the dissolved oxygen in the melt is in equilibrium with the oxygen in the gas phase:

$$\frac{1}{2}\text{O}_2(g) = \underline{O}, (\Delta G_2^0 = -115750 - 4.63T = -19.142 \cdot T \cdot \log \frac{f_O \cdot [O\%]}{p_{O_2}^{(syst)1/2}}) \quad (2)$$

where  $f_O$  is the 1 wt-% oxygen activity coefficient and  $\Delta G_2^0$  is expressed in J<sup>12</sup>, from which  $p_{O_2}^{syst}$  can be calculated. Finally, the Gibbs free energy change for the  $\text{FeO}$ -decomposition reaction is:

$$\Delta G_1 = \Delta G_1^0 + RT \ln \frac{a_{Fe} p_{O_2}^{(syst)1/2}}{a_{FeO}}$$

Because of lack of experimental data for the system  $\text{Mg-Al-Cr-Fe-O}$ ,  $f_{FeO}$  was assumed to be equal to the  $\text{FeO}$  molar fraction (0.08). The  $f_{Fe}$ -value was assumed to be unity. The chemical condition was calculated (**Fig. 5**) via the method described above. The calculated oxygen partial

pressure ( $p_{O_2}^{syst}$ ) is between  $10^{-14}$  and  $10^{-9}$  atm, depending on the specific VOD-stage. It is meaningful to stress that the calculated oxygen partial pressure must be seen as an average and representative oxygen potential for the liquid phases in the ladle. From a chemical point of view, the decomposition reaction is possible during the entire VOD-process. However, when assessing the possibility of FeO-decomposition a distinction should be made between the chemical condition:

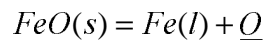
$$\Delta G_1 \leq 0 \text{ if } p_{O_2}^{refr,decomp} \geq p_{O_2}^{syst}$$

and the mechanical restriction which, in certain areas of the VOD-ladle, prevents the gaseous oxygen decomposition product to escape, preventing the reaction to proceed continuously:

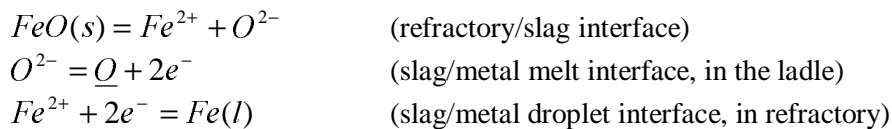
$$p_{O_2}^{refr,decomp} \ll p_{t,h} \quad (\forall h)$$

In principle,  $FeO_x$  of the refractory material in contact with liquid phases will not decompose as in reaction equation (1), due to this mechanical barrier<sup>§</sup>. The decomposition reaction would thus only be possible in the refractories just above the slag layer, as here only the chemical condition needs to be met. In practice however,  $FeO_x$ -decomposition was found in S4 and in S5 (both slag line refractories) but – although less severe – also as deep as 80 cm below the slag line refractories (e.g. in brick S3, see **Tables I and II**). There are several reasons, we believe, for this phenomenon.

- 1) Due to the turbulence in the ladle (Ar-,  $O_2$ -blowing) the impact zone (surface melt/refractory) shifts continuously.
- 2) Oxygen produced during the decomposition of  $FeO_x$  can be removed by rising (bottom blown) Ar- and CO-bubbles, allowing decomposition reaction (1) even far below the melt surface.
- 3) When slag infiltrates the brick, FeO may decompose, without the formation and removal of oxygen gas:



which will proceed in three steps:



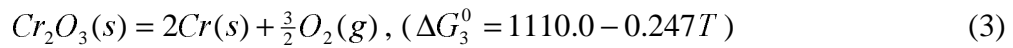

---

<sup>§</sup> The validity of the hypothesis of the effect of the ferrostatic pressure is supported by the observation that magnesia-carbon refractories in the VOD-ladle bottom are barely degraded, although it has been shown that in vacuum processes detrimental reactions between MgO and C may occur (forming Mg(g) and CO(g)). This hinders the successful use of magnesia-carbon refractories in ALZ's VOD-slag-line. However, in the ladle bottom these reactions are suppressed by the ferrostatic pressure.

The refractories several rows above the slag line (e.g. S6) do not show any  $\text{FeO}_x$ -decomposition. This can be explained as follows:

- 1) During the blowing stage the oxygen partial pressure in the gas phase contacting the refractories above the slag line, is higher than the oxygen partial pressure in the melt as calculated with the VOD-model, due to direct contact between the refractory and the top blown oxygen. In reality only 80% of the top blown oxygen reaches the melt directly.<sup>13</sup>
- 2) The temperature of the upper refractory layers is considerably lower than the temperature of the refractories in permanent contact with the liquid phases.

**Fig. 5** also shows the  $\text{Cr}_2\text{O}_3$ -decomposition, which can be calculated in a similar way as the  $\text{FeO}$ -decomposition ( $a_{\text{Cr}_2\text{O}_3} = 0.15$  and  $a_{\text{Cr}} = 1$ ):



where  $\Delta G_3^0$  is expressed in kJ.<sup>10</sup> From a chemical point of view,  $\text{Cr}_2\text{O}_3$ -decomposition is only possible during the reduction stage, whereas during the blowing and the degassing stage the inverse reaction may occur. Furthermore it is mostly during the blowing stage that the (slag line) impact zone varies continuously, allowing  $\text{FeO}_x$ -decomposition over a wide range of the refractory lining. Therefore, the metal particles in the worn bricks contain mainly Fe and only little Cr.

#### D. Changes in composition along the depth in the brick

$\text{FeO}_x$ -decomposition was observed in both the magnesia as in the chromite phases (see **Fig. 2**). The decomposition mechanisms of primary chromite are described in detail in a separate article.<sup>14</sup> To obtain an overall picture of the  $\text{FeO}_x$ -decomposition mechanisms in magnesia-chromite refractories, possible interactions between the chromite and the magnesia phases should also be investigated. For that reason, several measurements of the magnesia and secondary chromite phases (type I) were carried out along the depth (from the hot face to 4.5 cm in the brick) in a severely degraded brick (S4). The results for the magnesia phase are particularly interesting and are shown in **Fig. 6**. Before interpreting these results, it is useful to summarise the potential interactions between primary chromite, secondary chromite (type I and II) and magnesia at distinct temperatures. In the as-delivered material the  $\text{FeO}_x$ -content of the primary and the secondary spinel is respectively 13 wt-% and 20 wt-%. This difference is due to the higher MgO-affinity for  $\text{FeO}_x$  than for  $\text{Cr}_2\text{O}_3$  or  $\text{Al}_2\text{O}_3$ . During refractory production, surplus MgO diffuses into the chrome ore forming MgO-rich spinel while  $\text{FeO}_x$  and to a lesser extent  $\text{Cr}_2\text{O}_3$  and  $\text{Al}_2\text{O}_3$  are able to diffuse into the magnesia. After firing, the refractory is slowly cooled. As mentioned above, this results in a microstructure containing primary spinel (grain size > 200  $\mu\text{m}$ ), precipitation/exsolution of  $\text{FeO}_x$ -rich secondary spinel (type Ia, Ib and II), almost pure magnesia and some silicates ( $\text{C}_2\text{S}$  for the as-delivered brick). When this refractory is heated up during the VOD-process, the high temperature diffusion phenomena reoccur. Hence,  $\text{FeO}_x$  from the secondary chromite redissolves into the magnesia grains. After the end of the last VOD-process cycle (blowing, degassing, reduction stage, followed by stirring and continuous casting) the ladle is taken out of production. In this way, the refractory materials follow a cooling path and at the

surface of the brick this means that the material is effectively quenched. Therefore, the measured  $\text{FeO}_x$ -content in the magnesia at the hot face (surface) of the brick is an indication of the temperature of the liquid phases in direct contact with that refractory brick at that particular instance. Moreover, the temperature in a brick from a VOD-ladle is not uniform. The presence of a temperature gradient has important consequences on the interpretation of the EPMA-results. The sudden decrease in  $\text{FeO}_x$ -content in the magnesia at the hot face of sample S4, reflected as a marked increase in  $\text{FeO}$ -content in **Fig. 6** from 0 to 10 mm depth, is thus clearly the result of detrimental  $\text{FeO}_x$ -decomposition reactions. Hence, one can conclude that in the danger zones in the VOD-ladle (slag line refractories and upper layers in the metal bath),  $\text{FeO}_x$ -decomposition takes place at the surface of the refractory bricks. A continuous  $\text{FeO}_x$ -removal out of the refractory system becomes possible (see **Table 1** and **Fig. 4**). The magnesia-chromite refractories investigated in this paper are produced with South-African (Transvaal) chrome ores, that are low in  $\text{SiO}_2$  (1.8 wt-%) but rich in  $\text{FeO}_x$  (24.7 wt-%). The high  $\text{FeO}_x$ -content is thus a drawback of these refractory materials for this application.

#### E. Slag modification program

Slag infiltration into the refractory material and the subsequent dissolution of refractory-MgO into the infiltrated MgO-undersaturated slag contribute significantly to the degradation of the refractory lining. Therefore it was decided at ALZ to adjust the slag practice (targeting  $2\text{CaO}.\text{SiO}_2/\text{MgO}$  saturation) to minimise this effect. After a one-year trial period, it was concluded that the average VOD-ladle lining lifetime had increased by over 10 percent.<sup>15</sup>

### IV. SUMMARY AND CONCLUSIONS

The degradation mechanisms of direct bonded magnesia-chromite refractories in VOD-ladles were investigated. Severe refractory breakdown (**Fig. 7**) primarily occurs in the slag zone and in the top metal bath areas of the ladle, where some important conditions for degradation meet: prolonged turbulent contact slag/refractory, low oxygen partial pressure ( $p_{\text{O}_2}^{\text{syst}} \ll 0.001 \text{ atm}$ ) and high temperatures ( $> 1700^\circ\text{C}$ ). The influence of the ferrostatic pressure on the refractory degradation was shown.  $\text{FeO}_x$ -decomposition can occur in the magnesia and in the chromite phases, accelerating the degradation of the brick. As a result of this decomposition, the porosity increases allowing more slag infiltration. The latter is in effect the primary degradation mechanism. Liquid silicate slags infiltrate the refractory brick through the open pore network and the magnesia-grain boundaries. This process is enhanced as the bulk of the secondary chromite spinel is ‘inactivated’ at the high VOD-temperatures, due to diffusion mechanisms into surrounding magnesia (for type Ia chromite) or due to dissolution into the chrome-rich silicate liquid (for type Ib chromite). The infiltrated liquid also reacts with the magnesia phases forming low melting compounds such as CMS and  $\text{C}_3\text{MS}_2$ . At steelmaking temperatures, these phases are liquid. The normal direct bonding in the bricks is thus (partially) replaced by liquid bonding (chromia-rich silicate liquid). The turbulent bath movement in the VOD-ladles easily erodes such a system. This process is enhanced locally at the metal/slag interface, due to the Marangoni-effect. Furthermore, the densification of the hot face of the brick, due to severe slag infiltration, leads to high internal stresses between the infiltrated and the non-infiltrated zones. This results in discontinuous wear due to cracking and spalling. Finally, it was shown that the refractory



lifetime can be extended by improving the compatibility with the slag. The slag was therefore modified to target  $2\text{CaO}.\text{SiO}_2/\text{MgO}$  saturation.

## ACKNOWLEDGMENTS

Dr. E.B. Pretorius from Baker Refractories and Dr. W.E. Lee from the University of Sheffield are acknowledged for their useful comments on refractory wear and slag practice.

## REFERENCES

1. K. GOTO, W. E. LEE: *J. Am. Ceram. Soc.*, 1995, **78**, 1753-60.
2. J. MOSSER, G. BUCHEBNER, K. DÖSINGER: *Veitsch-Radex Rundschau*, 1997, **1**, 11-23.
3. R. ENGEL, R. MARR, E. PRETORIUS: *Iron and Steelmaker*, 1997, **24**, (4), 59-60.
4. J. WHITE: *Refractories J*, 1970, **46**, (11), 6-18.
5. W. HUANG, M. HILLERT and X. WANG: *Metall. Trans.*, 1995, **26A**, 2293-2309.
6. R. ENGEL, R. MARR, E. PRETORIUS: *Iron and Steelmaker*, 1997, **24**, (1), 48-49.
7. R.K. GHOSE, J. WHITE: *Trans. J. Brit. Ceram. Soc.*, 1980, **79**, 146-153.
8. W.E. LEE, S. ZHANG, *Int. Mat. Review*, 1999, **44**, (3), 1-28.
9. R. ENGEL, R. MARR, E. PRETORIUS: *Iron and Steelmaker*, 1997, **24**, (8), 57-58.
10. T. ABEL ENGH: 'Principles of Metal Refining', 407-425; 1992, Oxford, Oxford University Press.
11. R. DING, B. BLANPAIN, P.T. JONES, P. WOLLANTS: *Metall. Trans.*, 2000, **31B**, 197-206.
12. G.K. SIGWORTH, J.F. ELLIOTT: *Met. Sci.*, 1974, **8**, 298.
13. G. HEYLEN (ALZ-NV), private communication.
14. P.T. JONES, B. BLANPAIN, P. WOLLANTS, R. DING, B. HALLEMANS: *Ironmaking and Steelmaking*, in print (june 2000).
15. P.T. JONES, B. BLANPAIN, P. WOLLANTS, B. HALLEMANS, G. HEYLEN, J. WEY TJENS: *Iron and Steelmaker*, 1999, **26**, (12), 31-35.

## LIST OF FIGURES

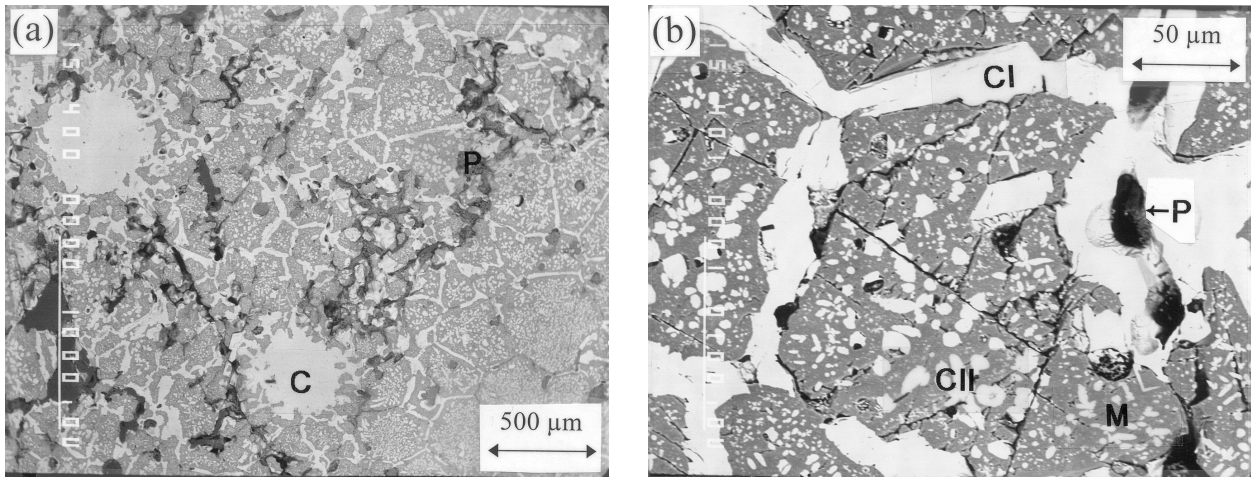


Fig 1 – Backscattered electron (BSE) micrographs (JEOL 733) showing the distribution of mineral grains (M = matrix, C = crystal, P = porosity) in a rock sample. The scale bar indicates 500 μm.

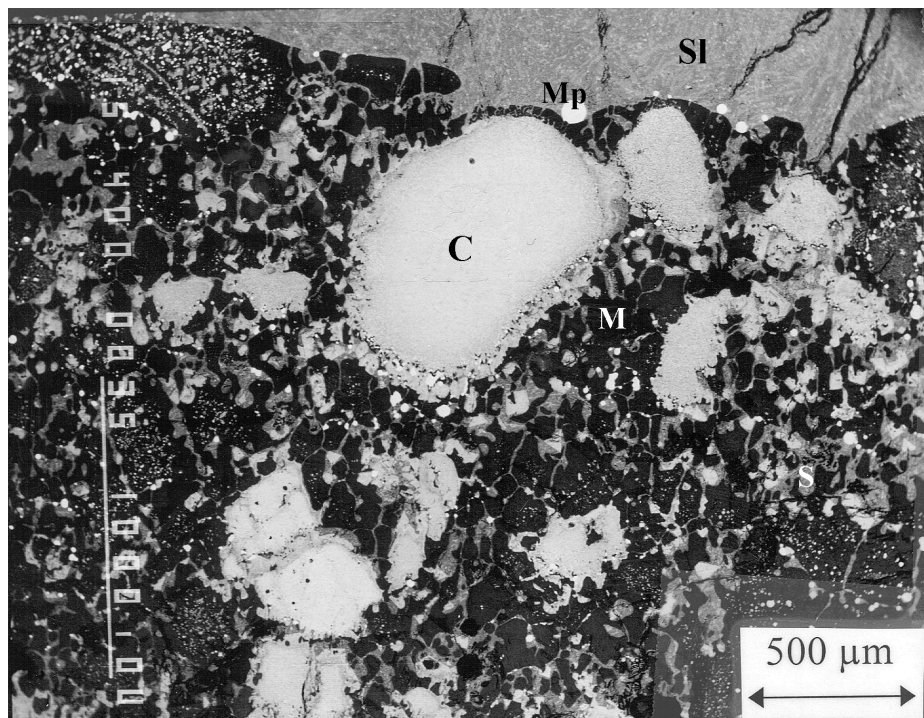


Fig 2 – Backscattered electron (BSE) micrograph (JEOL 733) showing the distribution of mineral grains (M = matrix, C = crystal, SI = silica) in a rock sample. The scale bar indicates 500 μm.

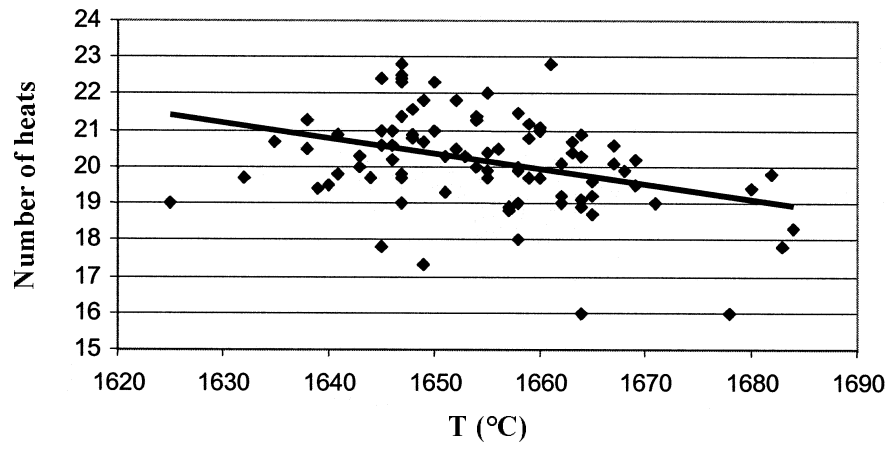


Fig 3 – Average primary metal temperature (°C) vs average number of heats

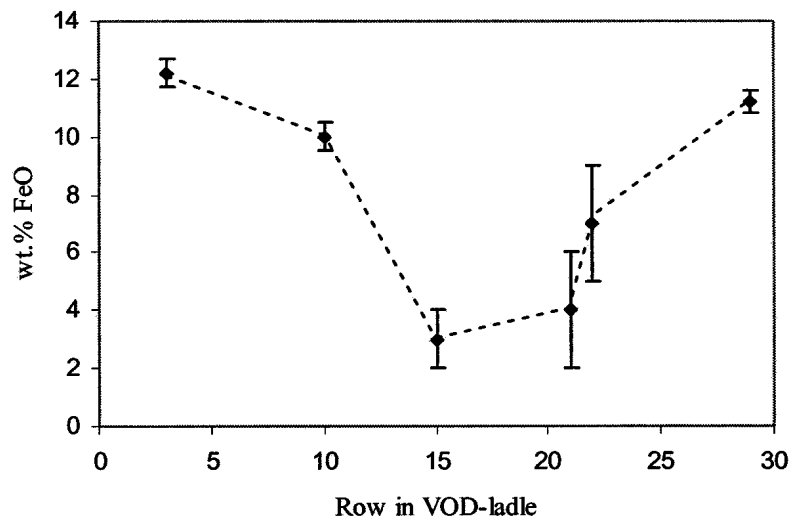


Fig 4 – Overweight FeO contents in samples 1, 2, 3, 4, 5 and 6, determined by EPMA E (JEOL 733), shown in the O.D.

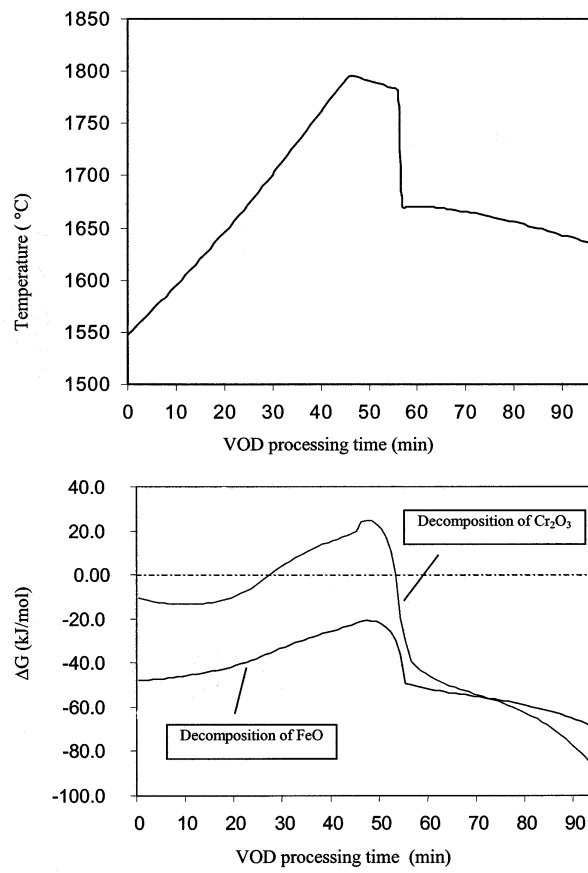
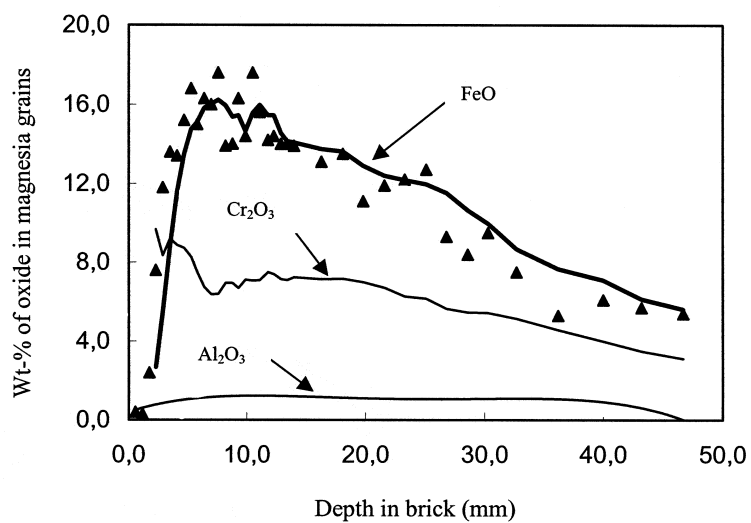
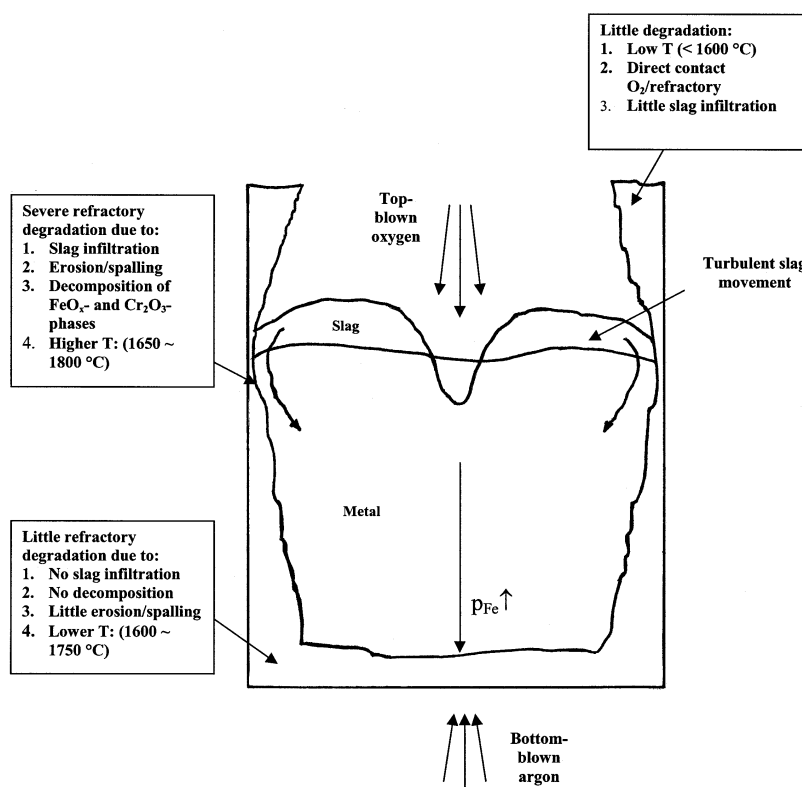


Fig 5 – Calculated temperature,  $\Delta G_1$  and  $\Delta G_3$  vs VOD processing time

$$a_{FeO} = 0.08 \quad a_{Cr_2O_3} = 0.15 \quad a_{Fe} = 0.9 \quad a_{Cr} = 0.9$$



a a a a a a a a



a a a a a a a a

## LIST OF TABLES

*a*                      *a*                      *a*                      *a*                      *a*

*a*                      *a*

Brick number	Row number in VOD-ladle	Position in VOD-ladle	Remaining thickness of brick (cm)	FeO-content at the hot face (global EPMA-EDS analysis)
S1	3	Steel bath	6 - 8	12.2 ± 0.5*
S2	10	Steel bath	7	10.0 ± 0.5
S3	15	Steel bath	4 - 4.5	3 ± 1
S4	21	Slag area	3 - 4	4 ± 2
S5	22	Slag area	3 - 3.5	7 ± 2
S6	29	Above slag area	4 - 5	11.2 ± 0.4

\* standard deviation (based on 6 measurements)

*a*                      *a*      *a a*                      *a*      *a*

*a*      *a*                      *a %*

Refractory brick	Row number in ladle	Main Features		
		Slag infiltration	Metallic particles	Decomposition of primary chromite
S1	3 (bottom steel bath)	Local (0-2 mm) CMS/C <sub>3</sub> MS <sub>2</sub> *	None	None
S2	10 (middle steel bath)	Deeper (0-2 cm) CMS/C <sub>3</sub> MS <sub>2</sub>	None	None
S3	15 (top steel bath)	Strong (entire remaining brick) CMS (surface) CMS/C <sub>3</sub> MS <sub>2</sub> (deeper)	Many (hot face) (90 Fe, 10 Cr)	Strong (hot face)
S4	21 (slag area)	Very strong (entire remaining brick) CMS (surface) CMS/C <sub>3</sub> MS <sub>2</sub> (deeper)	Many (hot face) (90 Fe, 10 Cr)	Very strong (hot face)
S5	22 (slag area)	Strong (entire remaining brick) CMS (surface) CMS/C <sub>3</sub> MS <sub>2</sub> (deeper)	Many (hot face) (90 Fe, 10 Cr)	Strong (hot face)
S6	29 (above slag area)	Local (0-2 mm) C <sub>3</sub> MS <sub>2</sub>	None	None

\* CMS = CaO.MgO.SiO<sub>2</sub> (monticellite), C<sub>3</sub>MS<sub>2</sub> = 3CaO.MgO.2SiO<sub>2</sub> (merwinite), C<sub>2</sub>S = 2CaO.SiO<sub>2</sub> (dicalcium silicate)

